ELSEVIER

Forced-air precooling of spherical foods in bulk: A parametric study

B. Sadashive Gowda, G. S. V. L. Narasimham and M. V. Krishna Murthy
Department of Mechanical Engineering, Indian Institute of Science, Bangalore, India

In this paper, a mathematical model for forced-air precooling of spherical food products in bulk is developed. The foods are arranged in horizontal layers stacked one above the other to form a rectangular parallelepiped with a vertical gap in between the product layers. The foods are cooled by chilled air blown along the height of the package. The governing equations for the conduction heat transfer in the foods, simultaneous heat and mass transfer at the food–air interface and in the air stream are solved numerically using finite-difference methods. A comprehensive numerical study is performed by varying the process parameters over a wide range. Typical results showing the variation of moist air properties along the height of the package and the effect of each parameter on the process time are presented. The ranges of parameters for advantageous operation of the precooling system are identified. Correlations are obtained for the process time based on the product center and mass-averaged temperatures in terms of process parameters.

Keywords: forced-air precooling; heat and mass transfer; foods in bulk

Introduction

It is known that perishable produce decays rapidly when stored at ambient temperature because of the peak activity of decay-causing pathogens and higher metabolic activity. High storage temperatures also cause higher moisture loss and hence, wilting of the produce, because of increased vapour pressure difference between the product surface and the air in the storage space. It is also known that these undesirable effects are reduced considerably at lower temperatures, thus prolonging shelf life of produce. Precooling is the rapid removal of field heat immediately after the harvest of the produce, prior to transportation or storage, and is the first operation in the cold chain. Various types of precooling techniques, such as ice cooling, air cooling, hydrocooling, and vacuum cooling are used to lower the temperature of foodstuffs, and these techniques are described in detail by Hall (1974) and ASHRAE (1994). The importance of heat and mass transfer in precooling processes has been reviewed by Badarinarayana and Krishna Murthy (1976) and Gaffney et al. (1985a).

Mathematical models proposed in the literature for predicting the precooling characteristics of a single or an isolated food product range from the usual lumped system models subjected to convective heat transfer at the surface to more rigorous models, which consider coupled heat and mass transfer inside the product (Luikov 1975; Rossen and Hayakawa 1977).

Foods such as fruits and vegetables usually contain more than 90% water and may also be subjected to a prewetting process before precooling. Both these factors require that the moisture loss be properly taken into account. Hence, the simple models, which neglect moisture loss, cannot give completely satisfactory results.

Although Dyner and Hesselschwerdt (1964) took evaporation of moisture from the surface of the foods into account, in their mathematical model, the air used for precooling is assumed to be saturated. Sreenivasa Murthy et al. (1974, 1976), while accounting for heat and mass transfer at the product surface, implicitly assume that the lowest temperature to which the foods can be cooled is only the dry bulb temperature (DBT) of the surrounding air. This analysis has been subsequently modified by Badarinarayana and Krishna Murthy (1979a, 1979b) and Abdul Majeed et al. (1980), and these analyses correctly predict the lowest temperature to which the products can be cooled to be the wet bulb temperature (WBT) of the surrounding air. However, all of these models are applicable to an isolated single product and are invalid for cooling of food products in bulk because of differences in heat and mass transfer coefficients and warming up of the cooling medium as it flows through the package.

Some studies do exist that attempt to investigate the precooling characteristics of bulk loads of foods using simplified analyses, but their attention is focused on obtaining temperature data for the air side of the package (Holdredge and Wyse 1982; Misener and Shove 1976) or the mass transfer from the surface of the food products is neglected entirely (Baird and Gaffney 1976).

Here, we attempt to simulate the forced-air precooling of foods in bulk. The mathematical model developed includes a number of additional features, such as the temperature and humidity variation of air along the height of the package, two-dimensional (2-D) heat flow in the product with internal heat generation, and simultaneous heat and mass transfer at the product surface.

Address reprint requests to Prof. M. V. Krishna Murthy, Department of Mechanical Engineering, Indian Institute of Science, Bangalore 560 012, India.

Received 31 January 1996; accepted 3 February 1997

Int. J. Heat and Fluid Flow 18: 613–624, 1997

655 Avenue of the Americas, New York, NY 10010

0142-727X/97/$17.00
PII S0142-727X(97)00028-3

Theoretical analysis

Physical model

The physical model consists of a number of food and air layers in sequence in the form of a rectangular parallelepiped (Figure 1). The spherical geometry of the food is chosen, because many fruits and vegetables can be approximated satisfactorily by this shape. The foods are packed in horizontal layers, with an air gap between the layers to facilitate easy loading and unloading of the foods. If R is the radius of the product and I is the height of the air gap, the overall height of the package H, containing L product layers will be equal to $L(2R)+(L-1)I$, as shown in Figure 1. The void fraction of a product layer depends upon the number of foods in the layer, varying from 0.48 when the foods are tightly packed to 0.99 when only a single food stands in the layer. For the results in this paper, each food layer is assumed to have the same void fraction, and the height of the air gap is chosen to be equal to the radius of the product. The validity of these assumptions becomes obvious later.

A spherical coordinate system is employed for the food, with the radial coordinate r measured from the center of the food, and a Cartesian coordinate system is used for the air flow, with the z-coordinate measured from the bottom of the package. Initially, all the foods in the package are assumed to be at uniform temperature T_{po}. The foods are cooled by chilled air that enters the package at the bottom (i.e., $z=0$). The foods generate respiration heat, which is a function of temperature as given later by Equation 4. The conditions of air at the entry to the package are assumed to be constant.

Mathematical formulation

The governing equations for the food and the moist air are written with the following assumptions.

(1) The food is homogeneous and isotropic.
(2) Thermophysical properties of the food, such as specific heat, thermal conductivity, and thermal diffusivity are temperature-independent.
(3) Moisture concentration gradient and the evaporation within the product are neglected (Soule et al. 1966).
(4) The product temperature is invariant in the azimuthal direction.
(5) Air temperature and humidity ratio vary only in the z-direction (perfect radial mixing).
(6) The thermophysical properties of moist air are invariant with temperature (because the temperature range involved in precooling practices is small, rarely exceeding 30°C even in the tropics).
(7) Radiative heat transfer is negligible in view of the low ranges of temperatures encountered in precooling practice.

To obtain the solution in a generalized form that is applicable to a wide variety of products and processing conditions, the

Notation

a	thermal diffusivity, m^2s^{-1}
A_{psu}	food surface area available per unit volume of the package, m^2m^{-3}
A_0, A_1, A_2	coefficients defined in Equation 13
Bi	Biot number
C_0, C_1, C_2	coefficients defined in Equation 20
C_p	specific heat, $Jkg^{-1}K^{-1}$
d	diameter, m
D	binary diffusion coefficient of water vapor in dry air, m^2s^{-1}
D_1, D_2, D_3, D_4	coefficients defined in Equations 16–19, respectively
Fo	Fourier number (dimensionless)
$Fo_{p,c}$	process time based on food layers center temperature (dimensionless)
$Fo_{p,mav}$	process time based on mass average temperature (dimensionless)
g	acceleration because of gravity, ms^{-2}
Δh_v	enthalpy of evaporation, Jkg^{-1}
H	height of the package
I	height of the free layer
Ja	Jakob number (dimensionless)
L	number of food layers
Nu	Nusselt number (dimensionless)
Pr	Prandtl number (dimensionless)
q_{int}	heat of respiration of the food Wm^{-3}
r	radial coordinate, m
R	radius of the spherical food, m
Re	Reynolds number (dimensionless)
Sc	Schmidt number (dimensionless)
Sh	Sherwood number (dimensionless)
t	time, s
T	temperature, °C
T_{ma}	moist air dry bulb temperature at any z °C
w	velocity, ms^{-1}
W	humidity ratio, (kg/kg) dry air
z	coordinate along the height of the package measured from the bottom, m

Greek

α_h	heat transfer coefficient, $Wm^{-2}K^{-1}$
α_m	mass transfer coefficient, $kgm^{-2}s^{-1}$
θ	angular coordinate (dimensionless)
λ	thermal conductivity, $Wm^{-1}K^{-1}$
μ	dynamic viscosity, Nsm^{-2}
ν	kinematic viscosity, m^2s^{-1}
ρ	density, kgm^{-3}
ψ	void fraction (dimensionless)

Subscripts

c	center or cross section
e	entry
ma	moist air
mav	mass average
o	initial
p	product
pac	package
p,c	subscript used for dimensional process time
pp	total number of foods in the package
pl	total number of foods in the layer
ps	product surface
psu	per unit volume of the package
s	saturated, superficial
wb	wet bulb
wv	water vapor
da	dry air

Superscripts

*	dimensionless quantity

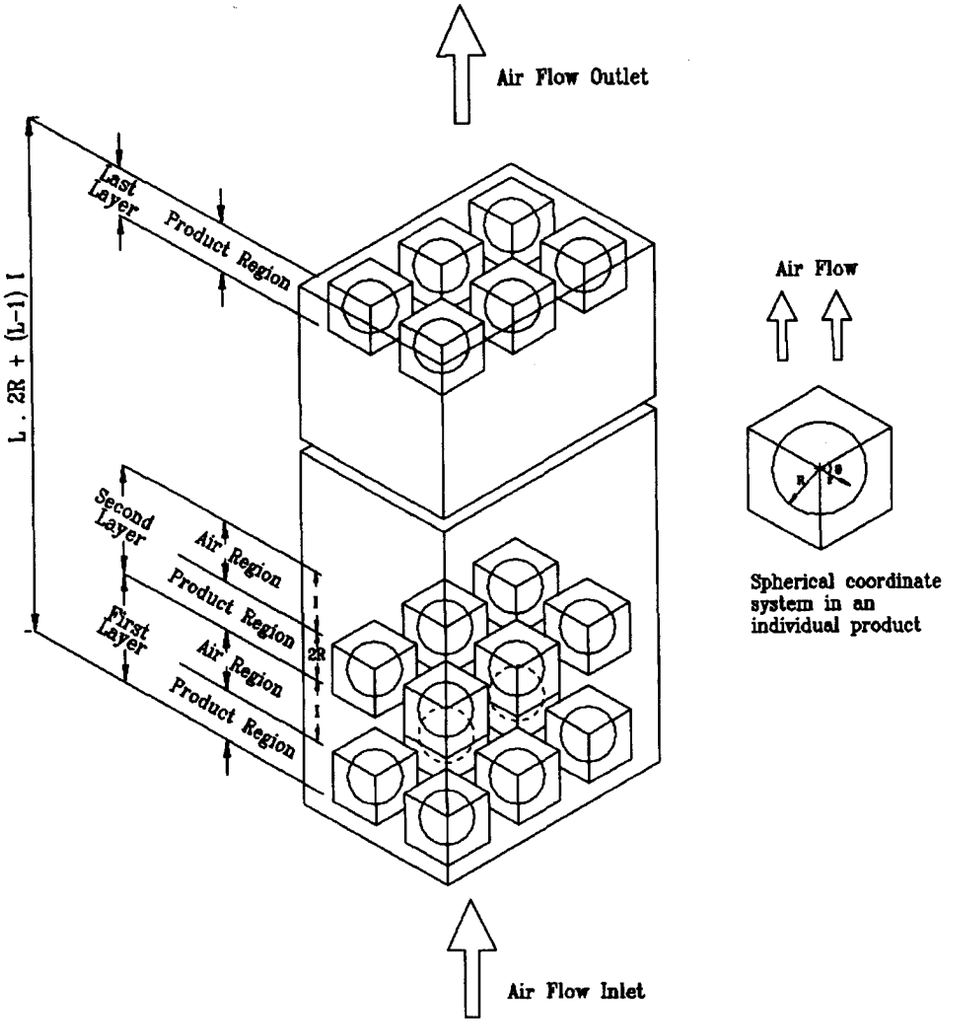

Figure 1 Physical model and co-ordinate system

following dimensionless parameters are defined:

$$T^* = \frac{T}{T_{po}}, \quad r^* = \frac{r}{R}, \quad H^* = \frac{H}{R}, \quad A^*_{\text{psu}} = A_{\text{psu}} R,$$

$$a^* = \frac{a_{\text{ma}}}{a_p}, \quad \lambda^* = \frac{\lambda_{\text{ma}}}{\lambda_p}, \quad q^*_{\text{int}} = \frac{q_{\text{int}} R^2}{\lambda_p T_{po}} \tag{1}$$

The following dimensionless parameters are obtained through nondimensionalization:

$$\text{Fo} = \frac{a_p t}{R^2}, \quad \text{Ja} = \frac{\Delta h_v}{C_{\text{pma}} T_{po}}, \quad \text{Re} = \frac{w_s (2R) \rho_{\text{ma}}}{\mu_{\text{ma}}}, \quad \text{Pr} = \frac{\nu_{\text{ma}}}{a_{\text{ma}}},$$

$$\text{Nu} = \frac{\alpha_h (2R)}{\lambda_{\text{ma}}}, \quad \text{Sc} = \frac{\nu_{\text{ma}}}{D_{\text{wvda}}}, \quad \text{Sh} = \frac{\alpha_m (2R)}{\rho_{\text{ma}} D_{\text{wvda}}} \tag{2}$$

Dimensionless governing equations

Product

The (2-D) transient heat conduction equation for the product in spherical coordinates is:

$$\frac{\partial^2 T^*_p}{\partial r^{*2}} + \frac{2}{r^*}\frac{\partial T^*_p}{\partial r^*} + \frac{\cot\theta}{r^{*2}}\frac{\partial T^*_p}{\partial \theta} + \frac{1}{r^{*2}}\frac{\partial^2 T^*_p}{\partial \theta^2} + q^*_{\text{int}} = \frac{\partial T^*_p}{\partial Fo} \tag{3}$$

where

$$q^*_{\text{int}} = A'(T^*_p + A'')^B \tag{4}$$

where

$$A' = \frac{\rho_p A R^2 T_{po}^{(B-1)}}{\lambda_p}; \quad A'' = \frac{17.8}{T_{po}} \tag{5}$$

The dimensional form of the internal heat generation q_{int} in Wm^{-3} is

$$q_{\text{int}} = \rho_p A (T_p + 17.8)^B \tag{6}$$

where T_p is the product temperature in °C, and A and B are constants for a given product. Gaffney et al. (1985b) have provided the values given in Table 1 for these constants for foods indicated for a temperature range of 0 to 27°C.

Moist air

(1) Energy equation:

$$\psi \frac{\partial T^*_{\text{ma}}}{\partial Fo} + \frac{1}{2}\text{Re}\,\text{Pr}\,a^* \frac{\partial T^*_{\text{ma}}}{\partial z^*} + \frac{\text{Sh}\,\text{Pr}\,A^*_{\text{psu}} a^*}{2Sc}$$

$$\times(W_{ps} - W_{ma})(T^*_{ps} - T^*_{ma})$$

$$= \psi a^* \frac{\partial^2 T^*_{ma}}{\partial z^{*2}} + \frac{1}{2}\mathrm{Nu}\, a^* A^*_{psu}(T^*_{ps} - T^*_{ma}) \quad (7)$$

The void fraction ψ is determined from the total volume of any food layer V_{total} and the volume V_{pl} of the foods contained in it, using the equation:

$$\psi = \frac{(V_{total} - V_{pl})}{V_{total}} \quad (8)$$

ψ assumes a value of 1.0 for the air layer; i.e., in between the product layers (this layer henceforth is referred to as the free layer). The third term on the left-hand side of Equation 7 results from the sensible cooling of water vapor from the temperatures of the evaporating surface to that of the adjacent moist air.

The energy source terms; i.e., the third term on the left-hand side and second term on the right-hand side of Equation 7 vanish for the free layer in between the product layers.

(2) Species (water vapour) conservation equation:

$$\psi \frac{\partial W_{ma}}{\partial Fo} + \frac{1}{2}\mathrm{Re}\,\mathrm{Pr}\, a^* \frac{\partial W_{ma}}{\partial z^*}$$

$$= \psi \frac{\mathrm{Pr}\, a^*}{\mathrm{Sc}} \frac{\partial^2 W_{ma}}{\partial z^{*2}} + \frac{\mathrm{Sh}\,\mathrm{Pr}\, a^* A^*_{psu}}{2\,\mathrm{Sc}}(W_{ps} - W_{ma}) \quad (9)$$

For the free layer, the second term on the right-hand side of the above equation vanishes, and ψ assumes a value of 1.0. It should be noted that in Equation 7, the contributions of the axial diffusion and the time-derivative terms become insignificant at higher values of Re Pr and Re Pr/H^*, respectively. Similar remarks also apply to Equation 9 for Re Sc.

Initial and boundary conditions

Product. For $\mathrm{Fo} \le 0, 0 \le r^* \le 1$ and $0 \le \theta \le \pi, T^*_p = 1.0$, symmetry of the temperature profile on vertical axis yields:
For $Fo > 0$:

$$\text{at} \quad \theta = 0 \quad \text{and} \quad \theta = \pi, \quad \frac{\partial T^*_p}{\partial \theta} = 0 \quad (10)$$

At $r^* = 0, T^*_p$ is finite.
At $r^* = 1.0$ and $0 < \theta < \pi$,

$$\frac{\partial T^*_p}{\partial r^*} = -\frac{\mathrm{Nu}\,\lambda^*}{2}(T^*_{ps} - T^*_{ma}) - \frac{\mathrm{Ja}\,\mathrm{Sh}\,\mathrm{Pr}\,\lambda^*}{2\,\mathrm{Sc}}(W_{ps} - W_{ma}) \quad (11)$$

Moist air. For $\mathrm{Fo} \le 0, 0 \le z^* \le H^*, T^*_{ma} = T^*_{mao}$.

For Fo > 0:

$$\text{at} \quad z^* = 0, \quad T^*_{ma} = T^*_{mae} \quad \text{and}$$

$$\text{at} \quad z^* = H^*, \quad \frac{\partial T^*_{ma}}{\partial z^*} = 0$$

Table 1 Constants in Equation 6 in the range 0–27°C

Apple	: $A = 4.59 \times 10^{-6}$ and $B = 2.66$
Peaches	: $A = 1.37 \times 10^{-7}$ and $B = 3.88$
Brussels sprouts	: $A = 4.87 \times 10^{-5}$ and $B = 2.47$

Species. For $\mathrm{Fo} \le 0, 0 \le z^* \le H^*, W_{ma} = W_{mao}$.

For Fo > 0:

$$\text{at} \quad z^* = 0, \quad W_{ma} = W_{mae} \quad \text{and}$$

$$\text{at} \quad z^* = H^*, \quad \frac{\partial W_{ma}}{\partial z^*} = 0$$

The saturated humidity ratio over the temperature range of 0 to 30°C taken from ASHRAE (1993) is correlated by the following equation:

$$W_{ps} = A_0 + A_1 T_s + A_2 T_s^2 \quad (12)$$

The linear regression of the data yielded the following values for constants A_0, A_1, and A_2 with a correlation coefficient of 0.999.

$$A_0 = 0.4206547 \times 10^{-2} \quad \text{(dimensionless)},$$

$$A_1 = 0.1077632 \times 10^{-3}\ K^{-1},$$

$$A_2 = 0.2153878 \times 10^{-4}\ K^{-2} \quad (13)$$

The WBT of the air at any point along the height of the package is found using the following implicit psychrometric relation (ASHRAE 1993).

$$W_{ma} = \frac{(2501 - 2.381T_{wb})W_s - (T_{ma} - T_{wb})}{2501 + 1.805T_{ma} - 4.186T_{wb}} \quad (14)$$

Nondimensionalization and rephrasing of Equation 14 yields:

$$D_1 T^{*3}_{wb} + D_2 T^{*2}_{wb} + D_3 T^*_{wb} + D_4 = 0 \quad (15)$$

where

$$D_1 = 2.381 C_2 T_{po} \quad (16)$$

$$D_2 = 2.381 C_1 T_{po} - 2501 C_2 \quad (17)$$

$$D_3 = 2.381 C_0 T_{po} - 4.186 W_{ma} T_{po} - T_{po} - 2501 C_1 \quad (18)$$

$$D_4 = 2501 W_{ma} + 1.805 W_{ma} T^*_{ma} T_{po} + T^*_{ma} T_{po} - 2501 C_0 \quad (19)$$

and with

$$C_0 = A_0, \quad C_1 = A_1 T_{po}, \quad C_2 = A_2 T^2_{po} \quad (20)$$

To calculate the heat and mass transfer coefficients for the food products, the entire package is assumed to form a packed bed. There are many correlations for evaluating heat and mass transfer in packed beds. For example, the correlations of Bird et al. 1960 (applicable for $0.35 \le \psi \le 0.94$, $\mathrm{Re} > 13$); Rowe and Claxton 1965 ($0.26 \le \psi \le 0.63$, $130 \le \mathrm{Re} \le 2000$), and Gnielinski 1981 ($0.26 \le \psi \le 0.94$, $1 \le \mathrm{Re} \le 10^5$), give, respectively, 87, 90, and 81 for Nu and 84, 87, and 77 for Sh, for the typical values of $\psi = 0.55$ and Re = 3400.

However, Gnielinski's correlation applies for wider ranges of Re and ψ and is found by Gnielinski to be in very good agreement with the experimental data from 21 independent sources, each covering a certain range of parameters. Furthermore, it combines the laminar and turbulent correlations into a single expression, which is applicable over the complete range of Reynolds number mentioned above. The theoretical basis for construction of such comprehensive correlating equations has been discussed by Churchill and Usagi (1972). Hence, Gnielinski's correlation is preferred in the present study, according to which the Nusselt number is given by the relation:

$$\mathrm{Nu} = f_{\psi_{pac}} \mathrm{Nu}_{\text{single sphere}} \tag{21}$$

where

$$\mathrm{Nu}_{\text{single sphere}} = 2 + (\mathrm{Nu}_{lam}^2 + \mathrm{Nu}_{turb}^2)^{0.5} \tag{22}$$

where

$$\mathrm{Nu}_{lam} = 0.664 \mathrm{Pr}^{1/3} \mathrm{Re}_{\psi_{pac}}^{1/2} \tag{23}$$

$$\mathrm{Nu}_{turb} = \frac{0.037 \mathrm{Re}_{\psi_{pac}}^{0.8} \mathrm{Pr}}{1 + 2.443 \mathrm{Re}_{\psi_{pac}}^{-0.1} (\mathrm{Pr}^{2/3} - 1)} \tag{24}$$

and

$$\mathrm{Re}_{\psi_{pac}} = \frac{w_s (2R)}{\nu \psi_{pac}} \tag{25}$$

The void fraction ψ_{pac} of the package is determined from the total volume (V_{pac}) of the package and the volume V_{pp} of the products contained in it using the Equation 26.

$$\psi_{pac} = \frac{V_{pac} - V_{pp}}{V_{pac}} \tag{26}$$

In Equation 21, $f_{\psi_{pac}}$ is the shape factor given by:

$$f_{\psi_{pac}} = 1 + 1.5(1 - \psi_{pac}) \tag{27}$$

The Sherwood number is evaluated in an analogous manner. The dimensionless mass average temperature of the food can be calculated using the following relation:

$$T^*_{mav} = \frac{3}{2} \int_{\theta=0}^{\pi} \int_{r^*=0}^{1} T_p^* r^{*2} \sin\theta \, dr^* \, d\theta \tag{28}$$

Method of solution

The above set of governing equations and nonlinear boundary conditions forms a complex mathematical problem, the solution of which cannot be obtained by analytical methods. Therefore, these equations are solved using finite-difference numerical techniques.

In view of the symmetry about the vertical axis, only a semicircle with a radius equal to that of the product can be considered as the computational domain. The computational domain and layout of the finite-difference grid are shown in Figure 2. For simplicity, only one food layer with the adjacent free air gap is shown in the figure. A nonuniform grid is adopted for the solution of the moist air equations for the product layer.

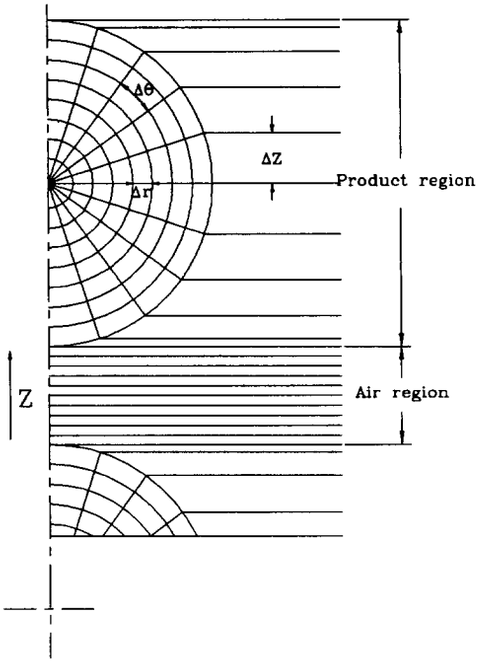

Figure 2 Finite-difference grid system for the product and air region

This nonuniform grid is obtained by horizontally extending the radial lines ending on the food surface. In the region between the food layers; i.e., the free layer, a uniform grid is chosen.

The Peaceman–Rachford alternating direction implicit (ADI) procedure (Peaceman and Rachford 1955) with forward time-centered space (FTCS) differencing is employed to advance the temperature in the product from time Fo to Fo + Δ Fo (that is, from time level n to $n + 1$). The ADI procedure accomplishes this task in two half-time steps. In the first half-time step, the equation is implicit in the r-direction, while in the second half-time step, it is implicit in the θ-direction, giving rise at each half-time step to a simple tridiagonal system of linear algebraic equations. These are solved using the Thomas algorithm (see, e.g., von Rosenberg 1969). The energy and species conservation equations are solved using the FTCS differencing, except for the convective terms, for which upwind differences are used (Roache 1982).

In view of the small temperature differences involved, the internal heat generation term in Equation 4 and nonlinear boundary condition at the food surface Equation 11 is linearized, as is normally done for a radiation boundary condition (e.g., Carslaw and Jaeger 1959).

Because of the nonexistence of the radial symmetry at the center of the food, the radial gradient cannot be prescribed at the center. Therefore, to calculate the product center temperature, a local Cartesian mesh is used as employed by Hwang and Cheng (1970), the applicable equation being:

$$\frac{\partial T_p^*}{\partial \mathrm{Fo}} = \frac{\partial^2 T_p^*}{\partial X^{*2}} + \frac{\partial^2 T_p^*}{\partial Y^{*2}} + \frac{\partial^2 T_p^*}{\partial Z^{*2}} + q^*_{\text{int}} \tag{29}$$

The coordinates X, Y, and Z in the above equation are measured from the center of the spherical food. The discretized form of the above equation gives the center temperature in terms of the temperatures at its six nearest neighboring points, four of them (in the plane $\theta = \pi/2$) being equal. Thus, the center temperature can finally be related to the temperatures of

the neighboring points on the lines $\theta = 0$, $\theta = \pi/2$ and $\theta = \pi$. Some numerical experiments are performed to determine the grid size and the time-step for which the numerical solutions are stable and grid-independent.

Although implicit methods, which permit larger time-steps, are employed in the present study, it is often helpful to obtain a preliminary estimate of the time-step from criteria applicable to explicit methods. Linear stability analyses show that the explicit form of finite difference equations for the product, in the absence of the heat source term, are stable, provided that $\xi \leq 1$, where $\xi = V^{n+1}/V^n$ is the amplification factor, V being the amplitude function (see, e.g., Roache 1982). When a source term of the form shown in Equation 4 is present, the stability criterion for the explicit method should be modified to accommodate an exponential growth of temperature with time, which is the true solution. The modified criterion for stability states that (Richtmyer and Morton 1967; Smith 1985) $\xi \leq 1 + A'B(T^{*n}_{p,i,j} + A'')^{B-1}\Delta$ Fo, according to which the implicit methods are unconditionally stable, while the explicit methods should comply with the time-step restriction:

$$\Delta \text{Fo} \leq \frac{1}{2}\left[\frac{2\Delta r^{*2}}{4 + 4/(i-1)^2} + \frac{2(i-1)^2\Delta r^{*2}\Delta\theta^2}{4 + (j-1)^2\Delta\theta^2/\tan^2(j-1)\Delta\theta}\right] \tag{30}$$

where $i \geq 2$ and $j \geq 2$. The above restriction holds irrespective of the strength of the heat source, although for common fruits and vegetables, the contribution of the respiration heat is insignificant.

Various grids with the number of grid points ranging from 15 to 51 in the r-direction and from 17 to 53 in the θ-direction with time-steps of 0.0005, 0.001, 0.0025, 0.004, and 0.005 are examined. A total of 75 numerical experiments are performed to determine the grid size and the time-step. Finally, a grid size of 37×39 and a time-step of 0.001 have been found to give reasonably accurate results.

The time-steps chosen range from explicit limit to about 10 times as large. Although implicit methods, while being stable, may permit time-steps up to 50–100 times the explicit limit (see Pearson 1965), such large time-steps have not been used in the present study in the interest of preserving accuracy. The chosen grid size and time-step give 0.04% difference in process time, and changes in temperature are found only in the fourth decimal place when compared to a grid of 51×53 and time-step of 0.001. All of the computations are performed on the computer system CYBER 992. A typical run covering a Fourier number of 0.54 took about 3764 s of CPU time for a package of 50 food layers.

The nondimensionalization of the governing equations and the initial and boundary conditions show that the parameters governing the problem of heat and mass transfer in bulk air precooling are Re, λ^*, ψ, a^*, q^*_{int}, T^*_{mae}, T^*_{wbe}, and L as other independent parameters, such as the Pr, Ja, and Sc, become fixed for air–water systems. The parameters C_0, C_1, and C_2 become constant once the product initial temperature is specified; whereas, A^*_{spu}, Nu, and Sh are dependent parameters that can be calculated from the values of other independent parameters.

The thermophysical properties chosen for the product represent average values for a number of fruits and vegetables. The process conditions, namely, the entering air velocity, DBT, and WBT are selected based on values encountered in precooling practice. In addition, the parameters shown in Table 2 are held constant at the values indicated, and the properties of moist air are taken at a temperature of 10°C and a humidity ratio of 0.005 (RH 70%).

Table 2 Values of the parameters held constant

Product initial temperature, T_{po}	: 32°C
Free layer height, l	: 0.5d, m
Moist air Prandtl number, Pr	: 0.71
Moist air Schmidt number, Sc	: 0.56
Jakob number, Ja	: 76.6
Dimensionless cross-sectional area of the test section, A^*_c	: 400
Thermal conductivity of moist air, λ_{ma}	: 0.025, $\text{Wm}^{-1}\text{K}^{-1}$
Specific heat of moist air, C_{pma}	: 1010.2, $\text{Jkg}^{-1}\text{K}^{-1}$
Density of moist air, ρ_{ma}	: 1.24, kgm^{-3}
Kinematic viscosity of moist air, ν_{ma}	: 1.4184×10^{-5}, m^2s^{-1}
Coefficient of diffusion of water vapor in dry air, D_{wvda}	: 2.5201×10^{-5} $\text{m}^2\,\text{s}^{-1}$

The computer program is validated by reproducing results from the existing literature (Badarinarayana and Krishna Murthy 1979a).

Process time

Traditionally, quarter- ($\tau_{1/4}$) and half-cooling times ($\tau_{1/2}$) have been employed as quantitative measures of the cooling rates of foods (Thevenot 1955). Half-cooling time is defined as the time required to reduce the difference between food temperature (usually at the center) and the coolant temperature to half of the initial value. Quarter-cooling time can be defined similarly. Such definitions are suitable when the foods are subjected to pure convective cooling, because the cooling curves then approximate to a straight line when plotted on semilogarithmic coordinates. Thus, knowing either ($\tau_{1/4}$) or ($\tau_{1/2}$), the time required for any degree of cooling can be calculated using simple relations. When the foods are cooled by the combined action of sensible and latent heat transfers, as in the present case, the semilogarithmic plot of the cooling curve will not be a straight line. For this reason, a process time to characterize the cooling process is defined as below.

The process time is the time required for the difference between the product center temperature and inlet air WBT to reach 20% of the temperature difference between the food's initial temperature and the inlet air WBT. In other words, it is the time required for T^*_c to equal $(0.2 \pm 0.8T^*_{\text{wbe}})$. The dimensionless process time is denoted by $\text{Fo}_{p,c}$ and is used as a measure of the efficacy of the cooling process.

Because the foods in different layers in the package will have different cooling rates, the process time of each layer in the package will be different. The last layer, which takes the maximum time to reach the above prescribed temperature, is taken as the reference to define the process time for the entire package. Because some investigators (Smith and Bennett 1965; Baird and Gaffney 1976) have presented cooling curves of foods in terms of the mass average temperature (T^*_{mav}), the process time based on mass average temperature ($\text{Fo}_{p,\text{mav}}$), which is the time required for T^*_{mav} to equal $(0.2 + 0.8T^*_{\text{wbe}})$, is also determined for the purpose of comparison.

Results and discussion

The variation of center temperature and mass average temperature with time for foods in various layers for typical values of parameters are shown in Figures 3 and 4. Clearly, these curves exhibit a transient behavior typical to bodies subjected to cooling at the surface; namely, rapid cooling followed by leveling off of temperature at larger times. It can be seen that the first layer;

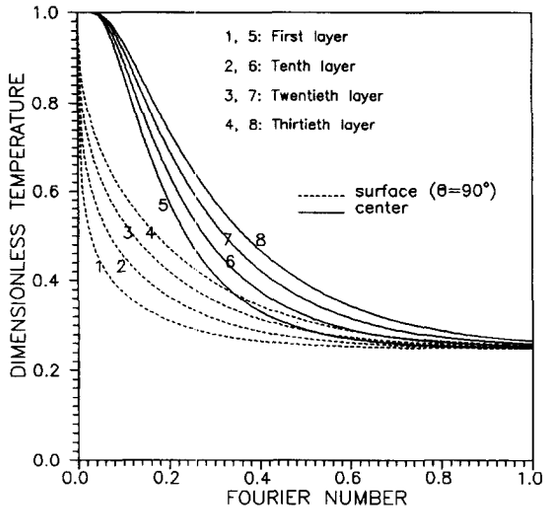

Figure 3 Typical cooling curves for product center and surface ($T_{po}=32°C$, $T^*_{mae}=0.3125$, $T^*_{wbe}=0.25$, Re=5287, $\psi=0.50$, $A=4.59\times10^{-6}$, $B=2.66$, $L=30$, $a^*=166$, and $\lambda^*=0.55$)

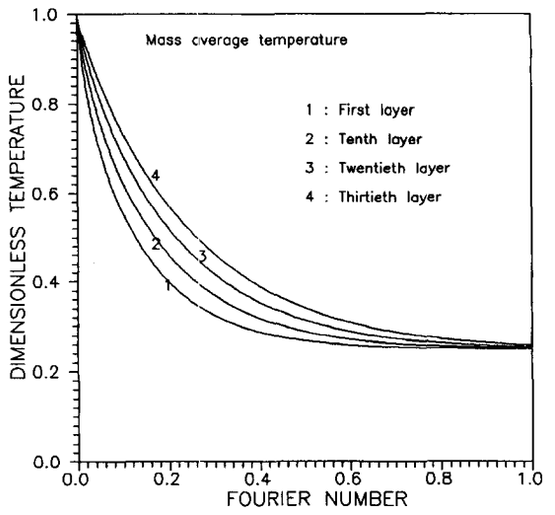

Figure 4 Typical variation of mass average temperature ($T_{po}=32°C$, $T^*_{mae}=0.3125$, $T^*_{wbe}=0.25$, Re=5287, $\psi=0.50$, $A=4.59\times10^{-6}$, $B=2.66$, $L=30$, $a^*=166$, and $\lambda^*=0.05$)

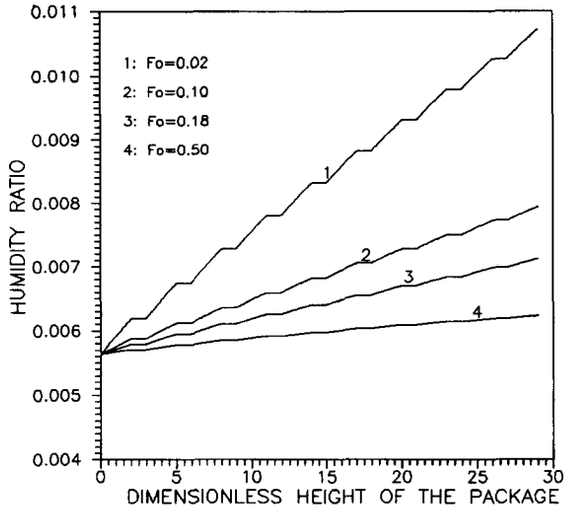

Figure 5 Variation of humidity ratio along the height of the package ($T_{po}=32°C$, $T^*_{mae}=0.3125$, $T^*_{wbe}=0.25$, Re=5287, $\psi=0.50$, $A=4.59\times10^{-6}$, $B=2.66$, $L=10$, $a^*=166$, and $\lambda^*=0.55$)

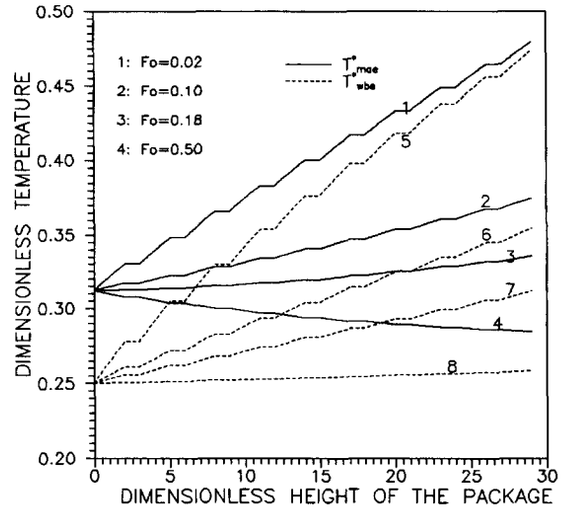

Figure 6 Variation of DBT and WBT along the height of the package ($T_{po}=32°C$, Re=5287, $\psi=0.50$, $A=4.59\times10^{-6}$, $B=2.66$, $L=10$, $a^*=166$, and $\lambda^*=0.05$)

i.e., the food layer nearest the entry of air, cools faster and reaches the lowest temperature; whereas, the last layer cools slower and is at the highest temperature in the package. The layers in between reach intermediate temperatures in ascending order from the first to the last.

Also of interest in bulk cooling are the variations of moist air properties; namely, humidity ratio, and dry and wet bulb temperatures along the height of the package. These are shown in Figures 5 and 6. Initially, the sensible heat transfer to adjacent air and evaporation from the surface of the foods take place at the expense of the internal energy of the foods. Hence, while the foods cool, the DBT increases all along the height of the package up to a certain Fourier number, depending upon the parameters chosen (Figure 6). If the surrounding air is saturated, the foods now reach a steady state, the potential for heat as well as mass transfer between the foods and the air having been reduced to null. On the other hand, if the surrounding air is unsaturated, as shown in Figures 5 and 6, further evaporation may occur by a decrease in the internal energy of the foods as well as sensible heat transfer from the surrounding air to the foods. Finally, the foods reach a steady state, in which the sensible heat transfer to the foods is balanced by the latent heat required for evaporation. Therefore, the DBT decreases with time all along the height of the package during later times (Figure 6). The humidity ratio and the WBT, however, continue to increase along the height of the package for all times (Figures 5 and 6), as can be expected. The reason the air temperature varies linearly as it passes through the product layers is because the surface area of a sphere increases linearly along any diametral axis. The DBT is found to be constant in the air gaps between the food layers.

Effect of Reynolds number on process time

When the Reynolds number is increased from 1700 to 12338 (corresponding to air velocities of ≈ 0.5 to 3.5 m/s), the process time decreases, as shown in Figure 7, because of enhancement in

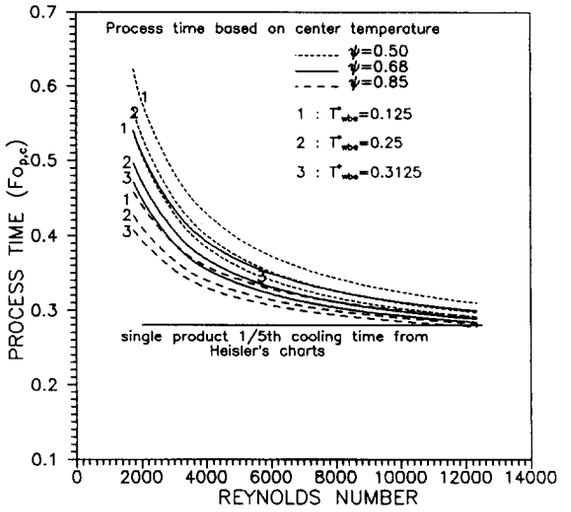

Figure 7 Effect of Reynolds number on process time (T_{po}= 32°C, T^*_{mae}=0.3125, $A=4.59\times10^{-6}$, B=2.66, L=30, a^*= 199, and λ^*=0.1)

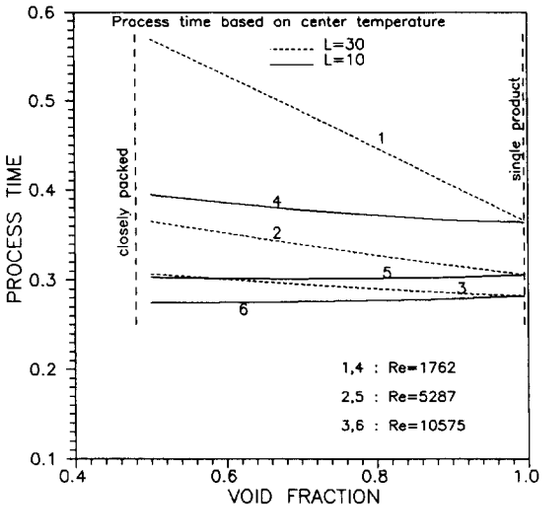

Figure 8 Effect of void fraction on process time (T_{po}=32°C, T^*_{mae}=0.3125, T^*_{wbe}=0.25, ψ=0.50, $A=4.59\times10^{-6}$, B= 2.66, a^*=199, and λ^*=0.05)

heat and mass transfer coefficients. However, this favorable effect begins to wear off at values of Re ranging from 5000 to 8000, for various combinations of parameters. Beyond this range, increasing the air velocity does not produce any substantial decrease in the process time. Therefore, it is advisable to operate the precooling plant at Re values ranging from 5000 to 8000 (i.e., 1.4 to 2.3 m/s), which is the most advantageous range. The flattening of the curves in Figure 7 is caused by the film resistances for heat and mass transfer becoming negligibly small at high values of Re, whence the enthalpy of air in contact with the food surface will be approximately equal to that of the adjacent air. In addition, if the DBT and WBT of the inlet air are equal, the food surface attains the temperature and humidity ratios of the adjacent air. The Heisler's charts can now be used to determine one-fifth of the cooling time, which, for zero surface resistance (i.e., $1/\mathrm{Bi}\to 0$), is found to be ≈ 0.28, as indicated in Figure 7. This is to be strictly compared with the one-fifth cooling time of the first layer for case $\psi=0.85$ (large void fraction) and $T^*_{mae}=T^*_{wbe}=0.3125$. Nevertheless, it can be seen that even the process time (i.e., one-fifth cooling time of the last layer) agrees well with this value.

Effect of void fraction on process time

The void fraction ψ is varied from 0.48 (corresponding to close packing of the layer; i.e., the foods touching one another) to 0.99 (corresponding to a single food standing in the layer). Increasing ψ has the effects of decreasing the food load and the surface area of the foods. Furthermore, the heat and mass transfer coefficients, in general, decrease with ψ, although less rapidly at lower Re. In discussing the effect of ψ on process time, it is important to consider the state of moist air adjacent to the foods in the last layer, and the rate of cooling of that governs the process time of the entire package, as mentioned earlier. At lower values of ψ, the heat and mass transfer coefficients are high. The air reaching the last layer has higher humidity ratio and temperature, and hence lower potential for heat and mass transfer. When ψ is increased, Nu and Sh decrease, and the air near the last layer has a greater potential for simultaneous heat and mass transfer, the food load decreasing at the same time. Therefore, the effect of ψ on process time is decided by the complex interaction among Nu and Sh, the state of air at the last food layer, and the food load. As shown in Figure 8, decrease in the load seems to outweigh other effects at lower values of Re, and process time is found to decrease with ψ, particularly when $L=30$. However, at higher values of Re, net change (either increase or reduction) in process time with ψ is not significant, whether $L=30$ or 10.

In practice, although the foods may tend to be packed randomly, the void fraction for each product layer still lies between the same two limits mentioned above, and its effect on the process time is not too large in this range, particularly at high-Reynolds numbers, which are typical for precooling operations. Furthermore, the variation of air gap height in the range $0<I<2R$ is found to affect the process time by less than 3%. Hence, it can be concluded that the results obtained here are applicable to practical precooling systems.

Effects of thermal conductivity and thermal diffusivity of the foods on process time

The effects of product thermal conductivity and diffusivity cannot be easily discerned by plotting the dimensionless process time $\mathrm{Fo}_{p,c}$ against a^*, because $\mathrm{Fo}_{p,c}$ itself contains a_p, which, in turn, contains λ_p. Hence, in Figures 9 and 10, $a^*\mathrm{Fo}_{p,c}$ (i.e., $a_{ma}t_{p,c}/R^2$) is shown plotted against $1/\lambda^*$ and $1/a^*$, respectively.

The product thermal conductivity is varied from 0.1 to 1.3 $\mathrm{Wm^{-1}K^{-1}}$. Figure 9 shows that an increase in thermal conductivity generally causes a decrease in the process time. However, values of $1/\lambda^*$ greater than about 30 do not result in any significant improvement in cooling. This is because the foods approach the behavior of a lumped system, where the foods' internal resistance becomes negligible, and the air-side heat and mass transfer coefficients alone govern the process time. The process times with the foods approximated by lumped systems are also shown in Figure 9. However, a simple calculation reveals that common fruits and vegetables undergoing air precooling (minimum $w_s\approx 1.5$ m/s, $\psi\approx 0.55$, D_p around 50 mm resulting in $\alpha_h\approx 55$ $\mathrm{Wm^{-2}K^{-1}}$, $\lambda_p\approx 0.4$ $\mathrm{Wm^{-1}K^{-1}}$) cannot be approximated by a lumped parameter model (i.e., the Biot number $\mathrm{Bi}\equiv\alpha_h D_p/(6\lambda_p)\approx 1.2$ is much larger than 0.1). The thermal conductivities of apples (0.418 $\mathrm{Wm^{-1}K^{-1}}$), grapes (0.464 $\mathrm{Wm^{-1}K^{-1}}$), tomatoes (0.61 $\mathrm{Wm^{-1}K^{-1}}$), and peaches (0.557 $\mathrm{Wm^{-1}K^{-1}}$) are indicated in Figure 9, from which it is clear that there are large differences in process times predicted by the

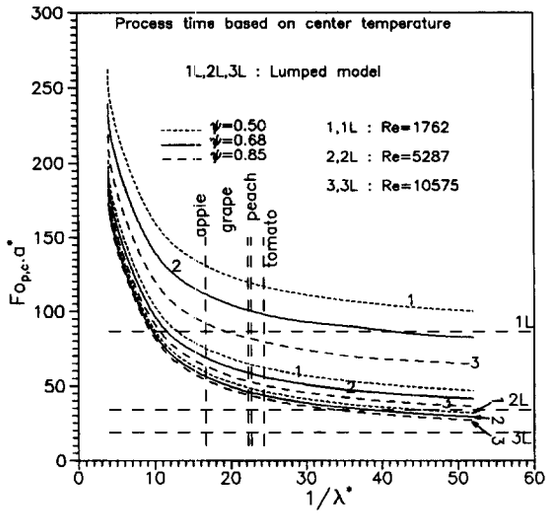

Figure 9 Effect of thermal conductivity on process time (T_{po}=32°C, T^*_{mae}=0.3125, T^*_{wbe}=0.25, $A=4.59\times10^{-6}$, B=2.66, L=30, a^*/λ^*=2796)

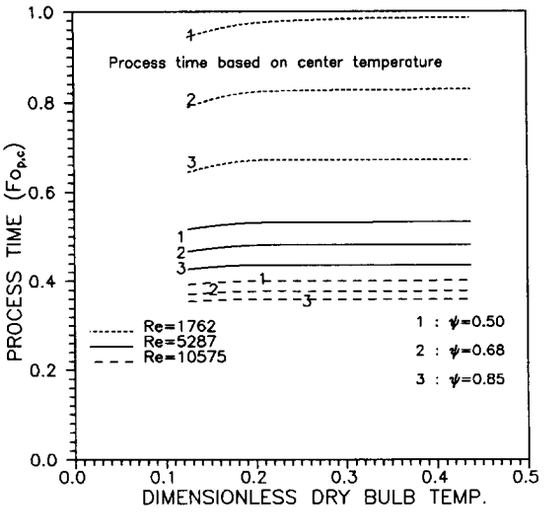

Figure 11 Effect of dry bulb temperature on process time (T_{po}=32°C, T^*_{wbe}=0.125, $A=4.59\times10^{-6}$, B=2.66, L=30, a^*=166, and λ^*=0.05)

distributed and the lumped parameter models. Figure 10 shows, as can be expected, that an increase in foods' thermal diffusivities results in reduced process time.

Effects of dry bulb and wet bulb temperatures on process time

As shown in Figure 11, an increase in the dry bulb temperature, while the wet bulb temperature is held fixed, causes a negligible change in the process time. This can be explained as follows. As the DBT is increased at constant WBT, the humidity ratio decreases; hence, the potential for mass transfer is increased. At the same time, the potential for sensible heat transfer between the products and the surrounding air is reduced. The net effect is that the potential for combined sensible and latent heat transfer is unaltered. Alternatively, it can be said that the enthalpy of the entering moist air remains almost unaffected, resulting in the above behavior.

From Figure 12, it appears that the process time decreases as the WBT is increased, while in reality, the opposite is the case. This ambiguity lies in the definition of process time. An examination of this definition reveals that the particular dimensionless product center temperature, at which the process time is assumed to have elapsed, itself depends upon the WBT. On the other hand, if the process time is defined in such a way that it is independent of the WBT, the expected trend can, indeed, be obtained. However, from the physics of the present problem, it is clear that the final steady-state temperature that can be attained by moist bodies such as foods corresponds to the WBT of the surrounding air. Hence, it is essential to base the definition of process time on the WBT of entering air.

Effect of the number of layers on process time

It can be seen from Figure 13 that the process time increases with increase in the number of food layers for any set of parameters. Two curves are shown in this graph, one pertaining

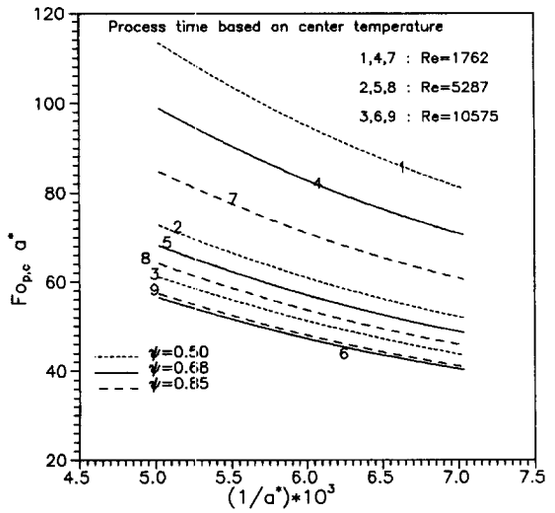

Figure 10 Effect of thermal diffusivity on process time (T_{po} =32°C, T^*_{mae}=0.3125, T^*_{wbe}=0.25, $A=4.59\times10^{-6}$, B=2.66, L=30, and λ^*=0.1)

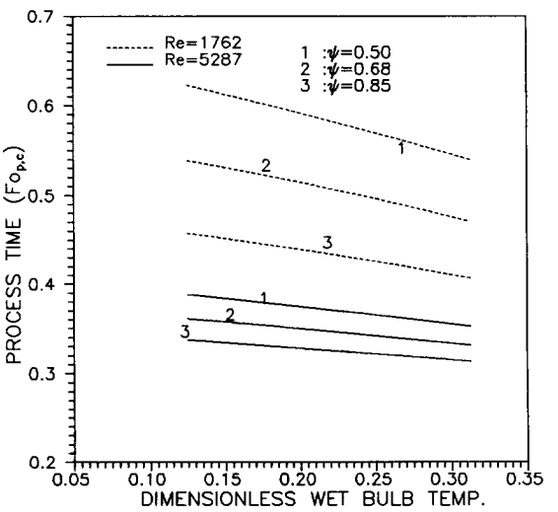

Figure 12 Effect of wet bulb temperature on process time (T_{po}=32°C, T^*_{mae}=0.3125, $A=4.59\times10^{-6}$, B=2.66, L=30, a^*=166, and λ^*=0.1)

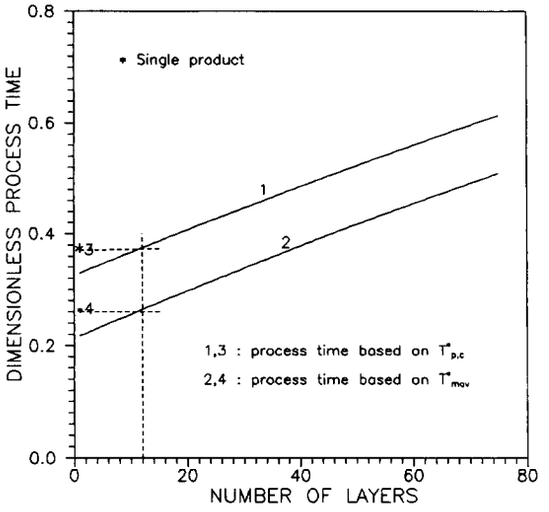

Figure 13 The variation of process time with number of layers (T_{po}=32°C, T^*_{mae}=0.3125, T^*_{wbe}=0.25, Re=5287, ψ=0.68, $A=4.59\times10^{-6}$, B=2.66, L=75, a^*=166, and λ^*=0.05)

to the process time based on the center temperature, and the other, based on the mass average temperature. For purposes of comparison, the process time of a single food is also shown. Bulk cooling can be seen, in fact, to be better than cooling of a single food until the layers increase to a certain number. This is because of better heat and mass transfer taking place in the package loaded with various foods, as compared to a single food. With a further increase in the number of layers, the air reaching the last layer becomes relatively warmer and more humid, and this becomes the governing factor for the process time, rather than the heat and mass transfer coefficients. Hence, beyond a particular number of layers, the process time for the package is higher than that for the single food. This particular number of layers, for typical parameter values used in forced-air precooling practice, is around 13, as can be seen from Figure 13.

The number of food layers cannot, of course, be increased indefinitely, because there comes a situation, where an extra layer added to the package would be unable to cool to the required storage temperature, however large the cooling time allowed might be. This threshold number of layers depends upon the parameters chosen. For the parameters shown in Figure 13, the threshold number of layers is found to exceed 75, the determination of the exact number itself requiring prohibitively large computing time.

Effect of respiration heat on process time

Equation 4 contains two parameters A and B, which are different for different products. The values of A and B are chosen in such a way that a wide variety of fruits and vegetables are covered. It is found that an increase in either A or B results in a marginal increase in process time, as shown in Table 3. Hence, it can be concluded that the respiration heat released has a negligible effect on the process time.

Correlation for process time

The following correlations for the dimensionless process times $Fo_{p,c}$ and $Fo_{p,mav}$, respectively, based on the center temperature and the mass average temperature, in terms of the process parameters, are obtained using multiple regression analysis:

$$Fo_{p,c} = a0\,Re^{a1}\psi^{a2}a^{*a3}\lambda^{*a4}T^{*a5}_{wbe}A^{a6}B^{a7}L^{a8} \tag{31}$$

$$Fo_{p,mav} = b0\,Re^{b1}\psi^{b2}a^{*b3}\lambda^{*b4}T^{*b5}_{wbe}A^{b6}B^{b7}L^{b8} \tag{32}$$

where the regression coefficients $a0$ to $a8$ and $b0$ to $b8$ are given below:

$a0 = 1.2434$,	$a1 = -0.3044$,	$a2 = -0.1045$,
$a3 = -7.7052\times10^{-3}$,	$a4 = -0.3703$,	$a5 = -0.1036$,
$a6 = 5.2149\times10^{-3}$,	$a7 = 0.0481$	and $a8 = 0.1023$.
$b0 = 1.2096$,	$b1 = -0.4160$,	$b2 = -0.1307$,
$b3 = -7.5844\times10^{-3}$,	$b4 = -0.5272$,	$b5 = -0.1460$,
$b6 = 4.976\times10^{-3}$,	$b7 = 0.0458$	and $b8 = 0.1434$.

These correlations are obtained using 1367 runs each with 30 food layers, yielding 41010 (= 1367 × 30) datapoints. From the regression analysis, the multiple correlation coefficient, standard error of estimate, and the percentage of error are found to be 0.949, 0.0975, 10.02, and 0.968, 0.1072, 7.99 for the above two correlations, respectively.

The correlation between the theoretical and correlated process times is shown in Figure 14, in which 2400 datapoints pertaining to the first and last layer only are shown to preserve clarity. With the remaining datapoints included, the correlation would, of course, look much better, but at the expense of clarity. The correlations developed above can be used to estimate the process time; i.e., the one-fifth cooling time, for given values of process parameters and the ranges of the parameters to be used are given in Tables 2 and 4.

Table 3 Process times

Sl. no.	Re	Process time ($Fo_{p,c}$) with heat of respiration		Process time ($Fo_{p,c}$) without heat of respiration	
		First layer	Last layer	First layer	Last layer
		$A=4.49\times10^{-6}$ and B=2.66			
1	1762	0.381611	0.883647	0.381047	0.880946
2	10575	0.285022	0.376249	0.284728	0.375726
		$A=1.37\times10^{-7}$ and B=3.88			
3	1762	0.382365	0.887058	0.381047	0.880946
4	10575	0.285422	0.376944	0.284728	0.375726
		$A=1.37\times10^{-7}$ and B=3.88			
5	1762	0.384085	0.895642	0.381047	0.880946
6	10575	0.286316	0.378548	0.284728	0.375726

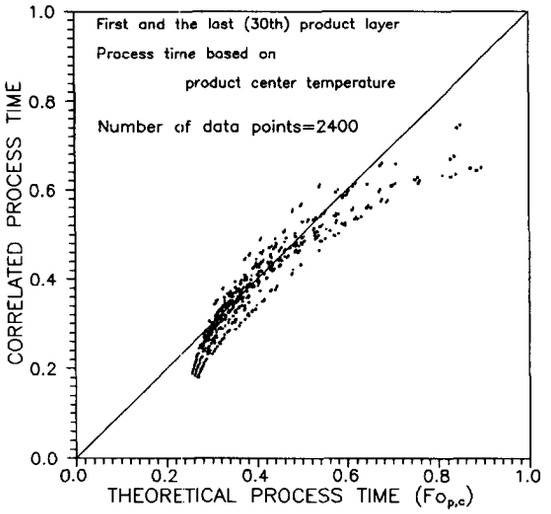

Figure 14 Comparison between theoretical and correlated process times

Table 4

Re	1762–12350
ψ	0.48–0.85
a^*	142–199 (i.e., 0.10×10^{-6}–0.14×10^{-6} $m^2 s^{-1}$)
λ^*	0.09996–0.02777 (i.e., 0.25–0.90 $Wm^{-1}K^{-1}$)
T^*_{wbe}	0.125–0.3125 (i.e., 4–10°C)
A and B	see Table 1
L	1–30

Conclusions

A mathematical model is developed to describe the simultaneous heat and mass transfer occurring during the bulk air precooling of spherical foods. The governing equations are solved using finite-difference numerical methods. A sensitivity analysis is performed to evaluate the effect of each parameter on process time. The main conclusions from the present investigation are as follows.

(1) The range of Reynolds numbers for the advantageous operation of the precooling system is found to be 5000–8000 (corresponding to air velocities $\approx$ 1.4 to 2.3 m/s), for the parameter values investigated.
(2) As the void fraction increases, the process time decreases at low-Reynolds numbers, but there is no substantial change in process time with void fraction at higher Reynolds numbers.
(3) An increase in thermal conductivity of the food results in lower process time (at very high values of λ_p, the lumped parameter model for product energy equation is found to predict process times reasonably accurately, although such high values are not characteristic of actual fruits and vegetables).
(4) During the relatively small periods of time employed for precooling (typically a few hours compared to days for storage), the heat of respiration does not have a significant effect on the process time.
(5) Increase in the thermal diffusivity of the foods results in lower processing time.
(6) The process time increases (almost linearly) with increasing number of food layers.
(7) The process times based on the center temperature and the mass average temperature are correlated in terms of the process parameters.

References

Abdul Majeed, P. M., Sreenivasa Murthy, S., and Krishna Murthy, M. V. 1980. Prediction of air-cooling characteristics of moist food products. *Trans. ASAE*, **23**, 788–792

American Society of Heating, Refrigerating, and Air Conditioning Engineers, Inc. (ASHRAE). 1993. *Handbook, Fundamentals*, SI Edition. (ASHRAE) Atlanta, GA

American Society of Heating, Refrigerating, and Air Conditioning Engineers, Inc. (ASHRAE). 1994. *Handbook, Refrigeration Systems, and Applications*. (ASHRAE) Atlanta, GA

Badarinarayana, K. and Krishna Murthy, M. V. 1979a. Heat and mass transfer characteristics and the evaluation of thermal properties of moist food materials. *Trans. ASAE*, **22**, 789–793

Badarinarayana, K. and Krishna Murthy, M. V. 1979b. Determination of thermal properties of food materials—Theory and experiments. *Wärme und Stoffübertragung*, **12**, 261–268

Baird, C. D. and Gaffney, J. J. 1976. A numerical procedure for calculating heat transfer in bulk loads of fruits or vegetables. *ASHRAE Trans.* **82**, 525–540.

Bird, R. B., Stewart, W. E. and Lightfoot, E. N. 1960. *Transport Phenomena*, Wiley, New York

Carslaw, H. S. and Jaeger, J. C. 1959. *Conduction of Heat in Solids*. 2nd ed. Clarendon, Oxford, UK

Churchill, S. W. and Usagi, R. 1972. A general expression for the correlation of rates of transfer and other phenomena. *AIChE J.*, **18**, 1121–1128

Dyner, H. and Hesselschwerdt, A. L., Jr. 1964. Temperature-time characteristics during food precooling. *Trans. ASHRAE* **70**, 249–255

Gaffney, J. J., Baird, C. D. and Chau, K. V. 1985a. Methods for calculating heat and mass transfer in fruits and vegetables individually and in bulk. *ASHRAE Trans.*, **91**, 333–352

Gaffney, J. J., Baird, C. D. and Chau, K. V. 1985b. Influence of airflow rate, respiration, evaporative cooling, and other factors affecting weight loss calculations for fruits and vegetables. *ASHRAE Trans.*, **91**, 690–707

Gnielinski, V. 1981. Equations for the calculation of heat and mass transfer during flow through stationary spherical packings at moderate and high peclet numbers. *Int. Chem. Eng.*, **21**, 378–383

Hall, E. G. 1974. Techniques of precooling: The long-term storage, controlled atmosphere storage, and freezing of fruits and vegetables. *Proc. Int. Seminar on Applications of Refrigeration to Vegetables, Fruits, and Fish in the Forest Region*, C.M.E.R.I., Durgapur, India

Holdredge, R. M. and Wyse, R. E. 1982. Computer simulation of the forced-convection cooling of sugarbeets. *Trans. ASAE*, **25**, 1425–1430

Hwang, G. J. and Cheng, K. C. 1970. Boundary vorticity method for convective heat transfer with secondary flow—Application to the combined free and forced laminar convection in horizontal tubes. *Proc. 4th Int. Heat Transfer Conference* (Paper NC 3.5) Paris-Versailles, Vol. IV, Elsevier, Amsterdam

Luikov, A. V. 1975. Systems of differential equations of heat and mass transfer in capillary-porous bodies (Review). *Int. J. Heat Mass Transfer*, **19**, 1–14

Misener, G. C. and Shove, G. C. 1976. Simulated cooling of potatoes. *Trans. ASAE*, **19**, 954–961

Peaceman, R. W. and Rachford, H. H. 1955. The numerical solutions of parabolic and elliptic equations. *J. Soc. Ind. Appl. Math.*, **3**, 28–41

Pearson, C. E. 1965. A computational method for viscous flow problems. *J. Fluid Mech.*, **21**, 611–622

Richtmyer, R. D. and Morton, K. W. 1967. *Difference Methods for Initial-Value Problems*, 2nd ed. Interscience, New York

Roache, P. J. 1982. *Computational Fluid Dynamics*, revised English ed. Hermosa Publishers, Albuquerque, NM

Rossen, J. L. and Hayakawa, K. 1977. Simultaneous heat and moisture transfer in dehydrated food: A review of theoretical models. *AIChE Prog. Symp. Ser.*, **73**, 71–81

Rowe, P. N. and Claxton, K. T. 1965. Heat and mass transfer from a single sphere to fluid flowing through an array. *Trans. Instn. Chem. Engrs.*, **43**, 321–331

Smith, G. D. 1985. *Numerical Solution of Partial Differential Equations —Finite Difference Methods*, 3rd ed. Clarendon, Oxford, UK

Smith, R. E. and Bennett, A. H. 1965. Mass-average temperature of fruits and vegetables during transient cooling. *Trans. ASAE*, **8**, 249–255

Soule, J., Yost, G. E. and Bennett, A. H. 1966. Certain heat transfer characteristics of oranges, grapefruit, and tangelos during forced-air precooling. *Trans. ASAE*, **9**, 355–358

Sreenivasa Murthy, S., Krishna Murthy, M. V. and Ramachandran, A. 1974. Heat transfer during air cooling and storing of moist food products. *Trans. ASAE*, **17**, 769–773

Sreenivasa Murthy, S., Krishna Murthy, M. V. and Ramachandran, A. 1976. Heat transfer during air cooling and storing of moist food products—II. Spherical and cylindrical shapes. *Trans. ASAE*, **19**, 577–583

Thevenot, R. 1955. Precooling. *Proc. 9th Int. Congress on Refrigeration*, Paris, Vol. 1, 51–77

von Rosenberg, D. U. 1969. *Methods for the Numerical Solution of Partial Differential Equations*. Elsevier, New York